Mathematical modeling of sintering of two cylinders in fused filament fabrication

Cite as: AIP Conference Proceedings **2289**, 020055 (2020); https://doi.org/10.1063/5.0028386
Published Online: 30 November 2020

Nickolas D. Polychronopoulos, and John Vlachopoulos

Mathematical Modeling of Sintering of Two Cylinders in Fused Filament Fabrication

Nickolas D. Polychronopoulos[1, a)] and John Vlachopoulos[2]

[1]*Polydynamics Inc., Dundas, ON, Canada*
[2]*Department of Chemical Engineering, McMaster University, Hamilton, ON, Canada*

[a)]Corresponding author: polyrheo@polydynamics.com

Abstract. In fused filament fabrication (FFF), it is important to know the time required for a pair of cylinders to coalesce and form a single cylinder. Virtually all present day mathematical models for viscous sintering of polymer particles are based on Frenkel's model, which was originally developed for the start of the coalescence. It is based on the assumption that the process time is determined by the balance of surface tension and viscous forces. The original model and subsequent modification, by the second author and coworkers, was for two spherical particles. In sintering of spheres the balance is carried out for a biaxial flow field. For cylinder sintering the flow field is planar. Frenkel's model has been modified for planar flow and extended to the completion of the process. Comparisons were made to an isothermal model presented by Hopper, where an inverse ellipse shape was used to describe the evolving geometry, rather that two intersecting cylinders of the present case. Comparison with some experimental data has also been carried out.
Keywords. coalescence, viscous sintering, neck growth, convexity

INTRODUCTION

The thermophysical interactions in additive manufacturing processes, such as Fused Filament Fabrication (FFF) and Selective Laser Sintering (SLS), are complex and intertwined. Simple mathematical models are necessary for a fundamental understanding of the processes. The first analytical work to describe the sintering of two isothermal viscous spherical particles (relevant to SLS), was carried out by Frenkel [1] and later corrected by Eshelby [2]. To describe the initial stage of isothermal sintering, the Frenkel Eshelby-corrected model assumes that the viscous dissipation balances the work done by surface tension. The balance is expressed mathematically as

$$W_V = W_S \tag{1}$$

where

$$W_V = \iiint_V \eta \nabla u : (\nabla u + \nabla u^T) dV \tag{2}$$

and

$$W_S = -\Gamma \frac{dS}{dt} \tag{3}$$

where η is the viscosity, V the volume of the sintering system, Γ the coefficient of surface tension, S the surface of the sintering system and ∇u the velocity gradient.

VISCOUS SINTERING MODEL OF A PAIR OF CYLINDERS

A model for sintering of a doublet of cylinders was proposed by Hopper [3]. In contrast to the biaxial flow field assumed by Frenkel-Eshelby for the doublet of spheres, Hopper's model assumes a planar flow, which is very close to what takes place in FFF. The model is based on the description of the cylinders doublet evolving cross section with a sequence of inverse ellipses. Martínez-Herrera and Derby [4] used two dimensional numerical simulations to study the sintering of two infinitely long cylinders. Their results are in agreement with Hopper's predictions. Kosztin *et al.* [5] proposed a model for sintering a pair of cylinders using the essential tenets of Pokluda *et al.* [6], assuming a planar flow field. The same lines were followed by Xu *et al.* [7]. Sintering of a doublet of cylinders has been also studied by Gurrala and Regalla [8], using the Pokluda *et al.* [6] model assuming a biaxial flow field.

The above-mentioned works do not provide enough information for the derivation of the neck growth equations and hardly any information on their importance in modeling the process of FFF.

Proceedings of PPS2019 Europe-Africa Regional Conference of the Polymer Processing Society
AIP Conf. Proc. 2289, 020055-1–020055-5; https://doi.org/10.1063/5.0028386
Published by AIP Publishing. 978-0-7354-4019-7/$30.00

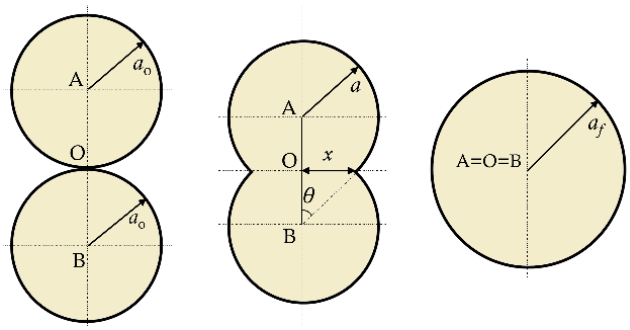

FIGURE 1. Schematic representation of the shape evolution of a pair of long cylinders of initial radius a_o. At some time t, the cylindrical parts intersect, forming a neck of width $x(t)$. The angle of intersection at that time is $\theta(t)$ and the radius $a(t)$. For simplicity the width, angle and radius are referred to as x, θ and a respectively. At the end of the process the final cylinder radius is $a_f > a_o$.

In sintering of spheres, it was assumed by Pokluda et al. [6] biaxial extensional flow. In sintering of cylinders the flow field is not biaxial, but planar described by

$$\nabla u = \begin{bmatrix} \dot{\varepsilon} & 0 & 0 \\ 0 & 0 & 0 \\ 0 & 0 & -\dot{\varepsilon} \end{bmatrix} \tag{4}$$

where $\dot{\varepsilon}$ is the elongation rate. Consequently, Eq. 2 takes the following form

$$W_V = \iiint_V 4\eta\dot{\varepsilon}^2 dV \tag{5}$$

At some time t, with reference to Fig. 1, the radius of each cylinder may be obtained from the conservation of mass (under the assumption of constant density) given by

$$a = a_o\left[\frac{\pi}{\pi - \theta + \sin\theta\cos\theta}\right]^{1/2} \tag{6}$$

For a doublet of filaments with length L, its total surface S may be calculated from

$$S = 4aL(\pi - \theta) \tag{7}$$

Substituting Eq. 6 into Eq. 7 results in

$$S = 4\pi^{1/2} L a_o \frac{\pi - \theta}{(\pi - \theta + \sin\theta\cos\theta)^{1/2}} \tag{8}$$

A constant elongation rate $\dot{\varepsilon}$ is assumed throughout the complete domain approximated by [6]

$$\dot{\varepsilon} = \frac{\partial u_y(B)}{\partial y} \approx \frac{u_y(B) - u_y(O)}{a} \tag{9}$$

At point O the velocity is zero, i.e. $u_y(O)$. The velocity $u_y(B)$ with which point B moves towards point O is given by

$$u_y(B) = \frac{dy}{dt} = \frac{d}{dt}(a\cos\theta) \tag{10}$$

Substituting Eq. 6 in Eq. 10 yields

$$u_y(B) = -\frac{\pi^{1/2} a_o(\pi - \theta)\sin\theta}{(\pi - \theta + \sin\theta\cos\theta)^{3/2}} \frac{d\theta}{dt} \tag{11}$$

Therefore, for the elongation rate $\dot{\varepsilon}$ we have

$$\dot{\varepsilon} = \frac{u_y(B)}{a} = -\frac{(\pi - \theta)\sin\theta}{\pi - \theta + \sin\theta\cos\theta} \frac{d\theta}{dt} \tag{12}$$

Substituting the above result in Eq. 5 we arrive at an expression for the dissipated energy

$$W_V = 8\pi L \eta a_o^2 \frac{(\pi - \theta)^2 \sin^2\theta}{(\pi - \theta + \sin\theta\cos\theta)^2} \left(\frac{d\theta}{dt}\right)^2 \tag{13}$$

A similar expression is derived for the work done by surface tension, substituting Eq. 8 in Eq. 3

$$W_S = 4\Gamma\pi^{1/2} La_o \frac{(\pi-\theta)\cos^2\theta + \sin\theta\cos\theta}{(\pi-\theta+\sin\theta\cos\theta)^{3/2}}\left(\frac{d\theta}{dt}\right) \tag{14}$$

Under the assumption of an always positive $d\theta/dt$, equating Eq. 13 with Eq. 14 results in

$$\frac{d\theta}{dt} = \frac{\Gamma}{a_o\eta} 2\pi^{-1/2} \frac{[(\pi-\theta)\cos\theta + \sin\theta](\pi-\theta+\sin\theta\cos\theta)^{1/2}}{(\pi-\theta)^2\sin\theta\tan\theta} \tag{15}$$

Note that in the limit as $\theta\to 0$ we have: $\pi-\theta\approx\pi$, $\sin\theta\approx\theta$, $\cos\theta\approx 1-\theta^2/2$ and $\tan\theta\approx\theta$. Therefore, Eq. 15 reduces to

$$\frac{d\theta}{dt} = 2\pi^{-1/2}\frac{\Gamma}{a_o\eta}\frac{1}{\theta^2} \tag{16}$$

which can be solved analytically giving

$$\theta = \left(\frac{3}{2\pi}\frac{t\Gamma}{a_o\eta}\right)^{1/3} \tag{17}$$

Eq. 17 may be regarded as a modified Frenkel model for sintering a pair of cylinders which applies at the start of the process. Eq. 15 is solved numerically following the lines by Pokluda *et al.* [6]. After θ is determined the dimensionless half neck width x/a_o is obtained from

$$x = a\sin\theta \tag{18}$$

or by substitution of Eq. 6 in the above

$$\frac{x}{a_o} = \sin\theta\left(\frac{\pi}{\pi-\theta+\sin\theta\cos\theta}\right)^{1/2} \tag{19}$$

RESULTS AND DISCUSSION

It is instructive to compare the numerical results for the sintering of a pair of cylinders (Eq. 15), with the corresponding model for sintering a doublet of spheres by Pokluda *et al*. [6]. At the early stage of the sintering process (Fig. 2a), the slope of the curve for the doublet of cylinders is higher than the one of spheres, which means that sintering of cylinders is faster than in the case of spheres. As the sintering time progresses (Fig. 2b), a cross-over point is observed (roughly when $\Gamma t/a_o\eta\approx 0.45$) after which the slope for sintering of spheres is higher than for cylinders, meaning spherical particles coalesce faster. At a later time, a second cross-over point is observed (approximately at $\Gamma t/a_o\eta\approx 7$) where the coalescence of spheres is nearly complete.

In Fig. 3 the predictions of the present model are compared to Hopper's [3] model. At the early stages of sintering, the present model predicts a faster sintering than Hopper's. After some time, there exists a cross-over point after which

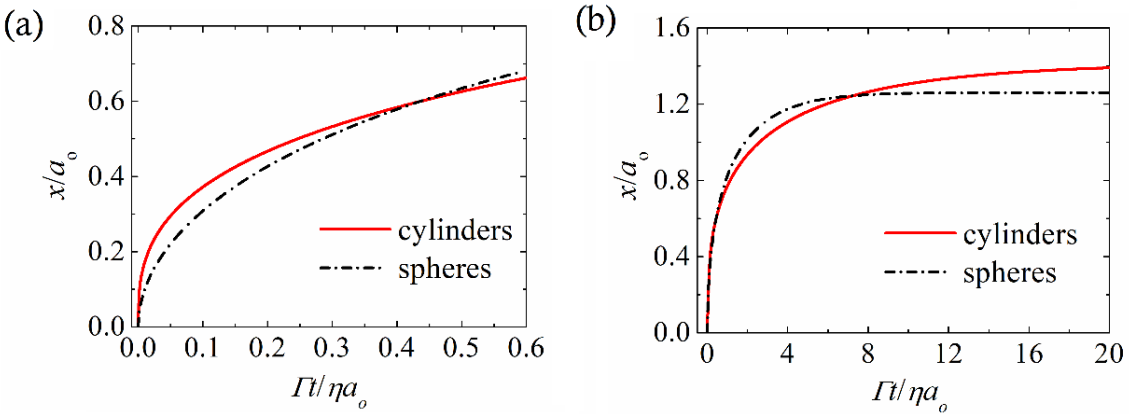

FIGURE 2. Comparison of the present model for a doublet of cylinders (Eq. 19) with that of spheres (Eq. 6) at (a) early sintering stage and (b) at later times.

Hopper's model predicts generally a faster coalescence. Full coalescence in Hopper's model is observed to be accomplished when the dimensionless time is about 5, whereas the present model predicts full coalescence when the dimensionless time is about 30. Such differences stem from differences of the curvature at the intersection of the

coalescing filaments. The present model assumes the intersection of two circles, while Hopper's model uses the inverse ellipse shape for the entire domain.

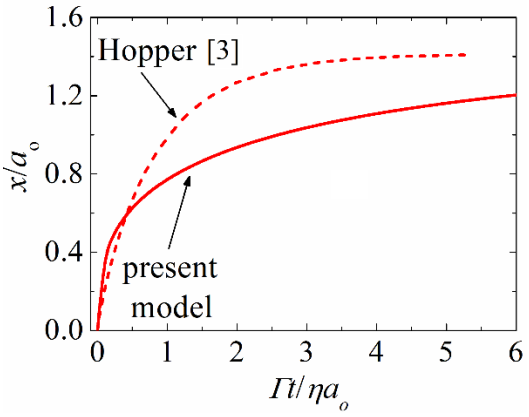

FIGURE 3. Comparison of the present model for cylinders with the model by Hopper [3], where the insert shows the value of the dimensionless neck width at full sintering.

Chaunier *et al.* [9] studied experimentally the isothermal sintering of a pair of cylinders at different temperatures. In their work they introduced the concept of the convexity index $I_{convex.}$, as a sensitive morphological descriptor to assess the quality of FFF. In Fig. 4a, the cross-sectional areas associated with the convexity index are shown. They define the convexity index as

$$I_{convex.} = \frac{S_1 + S_2}{S_1 + S_2 + S_3 + S_4} \tag{20}$$

where S_1=S_2 is cross-sectional area of the cylinders and S_3=S_4 corresponds to the formed concavities between the filaments. For I_{convex} reaching the value of 1, the bonding leads to a perfect fusion of the filaments without any residual concavity between them. In the present work, using simple geometrical considerations, an analytical expression for the area S_1 and S_2 is derived as a function of the bonding angle θ, given by

$$S_1 = a^2\left(\pi - \theta + \sin\theta\cos\theta\right) \tag{21}$$

The concavities S_3 or S_4 may be also expressed in a similar fashion

$$S_3 = a^2\left[2\cos\theta - (\pi/2) + \theta - \sin\theta\cos\theta\right] \tag{22}$$

An analytical expression for the convexity index may then be obtained

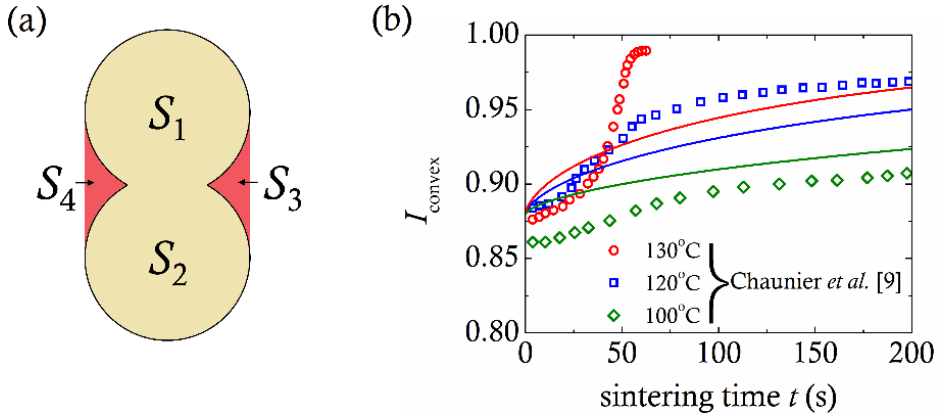

FIGURE 4. (a) Schematic representation of the cross-sectional areas associated with the convexity index ($I_{convex.}$) and (b) comparison of Chaunier *et al.* [9] experimental results of the convexity index with Eq. 23.

$$I_{convex.} = \frac{\pi - \theta + \sin\theta\cos\theta}{2\cos\theta + (\pi/2)} \tag{23}$$

Note that at θ=0 the convexity index is I_{convex}=$2\pi/(4+\pi)\approx 0.879$.

In Fig. 4b $I_{convex.}$ is shown as a function of sintering time, where θ is obtained from Eq. 15 and it is compared with the results from Chaunier *et al.* [9] for three different temperatures. For each temperature the temperature-dependent viscosity is calculated from [10,11]

$$\eta = \eta_o e^{-b(T-T_o)} \tag{24}$$

where η_o the viscosity at a reference temperature T_o and b is usually referred to as temperature sensitivity with units $^oC^{-1}$. Although, in [9] the authors report no rheological data, we obtained values from a past work by Chaunier *et al.* [12], assuming the material used is the same. In [11] the material has a zero-shear viscosity η_o=7000 Pa·s^n at T_o=130 ^{o}C. Assuming a typical b=0.05 $^oC^{-1}$, we calculate zero-shear viscosity 11541 Pa·s^n (at 120^{o}C) and 31371 Pa·s^n (at 100^{o}C). We also assume a typical value for the surface tension Γ=0.04 N/m. The filament radius is 1 mm in [9]. Our model predictions shown in Fig. 4b, capture the experimentally measured evolution of the convexity index qualitatively.

CONCLUDING REMARKS

The Pokluda *et al.* [6] model which accounts for the sintering process as two spheres form a larger one having a diameter 1.26 times larger than the initial, has been applied to two equal diameter cylinders. The model applies for the entire process of coalescence for the formation of a single cylinder having diameter 1.41 times larger than the initial. In both cases a homogeneous extensional flow field is assumed, biaxial for spheres and planar for cylinders. The sintering time for full coalescence, predicted by the present model of cylinders, is longer than that for spheres. The present model predicts somewhat different neck growth than a previous model by Hopper. The differences are apparently due to different shape of the cusp of the neck. The present model appears to be in qualitative agreement with some experimental data by Chaunier *et al.* [9].

REFERENCES

1. J. Frenkel, J. Phys., **9**, 385 (1945).
2. J.D. Eshelby, "Discussion" in A.J. Shaler, Metals Transactions, **185**, 796-813 (1949).
3. R.W. Hopper, Communications of the American Ceramic Society, **67**, C-262-C-264 (1984).
4. J.I. Martínez-Herrera and J.J. Derby, AIChE Journal, **40**, 1794-1803 (1994).
5. I. Kosztin, G. Vunjak-Novakovic and G. Forgacs, Rev. Mod. Phys., **84**, 1791-1805 (2012).
6. O. Pokluda, C.T. Bellehumeur and J. Vlachopoulos, AIChE Journal, **43**, 3253-3256 (1997).
7. F. Xu, X. Li, G. Regnier and D. Defauchy, Polymeric Materials Science and Engineering, **29**, 177-181 (2013).
8. P.K. Guralla and S.P. Regalla, Virtual and Physical Prototyping, 2014, **9**, 141-149 (2014).
9. L. Chaunier, G.D. Valle, D. Lourdin, A-L. Réguerre, K. Cochet and E. Leroy, Polym. Test., **77**, 105873 (2019).
10. J. Vlachopoulos and N. D. Polychronopoulos, Understanding Rheology and Technology of Polymer Extrusion, Polydynamics Inc, Dundas, Ontario, Canada (2019).
11. N. D. Polychronopoulos and J. Vlachopoulos, Polymer Processing and Rheology, Chapter 4, in M.A.J. Majumder, H. Sheardown, A. Al-Ahmed (Eds.), Functional Polymers, Springer, 133-180 (2019).
12. L. Chaunier, G.D. Valle, M. Dalgalarrondo, D. Lourdin, D. Marion and E. Leroy, Rheol. Acta, **56**, 941-953 (2017).